Lab on a Chip

Devices and applications at the micro- and nanoscale

Accepted Manuscript

This article can be cited before page numbers have been issued, to do this please use: H. Wang, H. Liu, Y. Song, X. Qin, Y. Li, K. Tang, H. Zheng, W. Xu, Z. Wang and B. Zhang, *Lab Chip*, 2025, DOI: 10.1039/D5LC00476D.

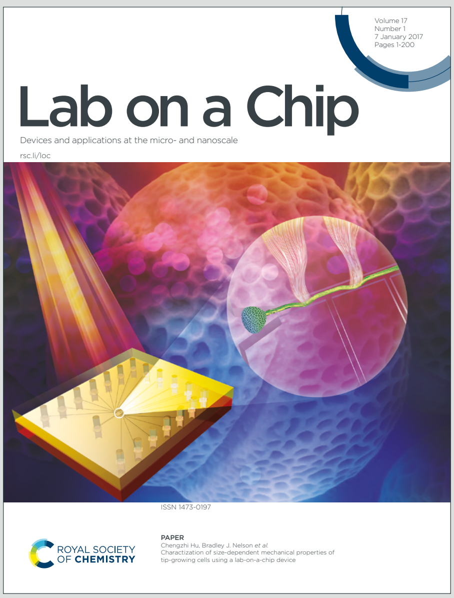

ROYAL SOCIETY OF CHEMISTRY

rsc.li/loc

View Article Online
DOI: 10.1039/D5LC00476D

ARTICLE

A hybrid flowing water-based energy generator inspired by rotatable waterwheel

Received 00th January 20xx,
Accepted 00th January 20xx

DOI: 10.1039/x0xx00000x

Hongbo Wang,[a] Hangchen Liu,[a] Yuxin Song,[a] Xuezhi Qin,[b] Yang Li,[b] Kairui Tang,[a] Huanxi Zheng,[c] Wanghuai Xu,[d] Zuankai Wang*[a] and Baoping Zhang*[a]

The ever-increasing global demand for low-carbon energy underscores the urgency of water energy harvesting. Despite intensive progress, achieving continuous and efficient water energy harvesting — particularly from abundant, distributed, and low-frequency water flows such as rain, streams, and rivers — remains a critical challenge. Herein, inspired by the classical waterwheel that spatially decouples the gravitational force of flowing water into orthogonal directions for continuous rotation, we report a hybrid, rotatable flowing water-based energy generator (R-FEG) capable of continuous and efficient water energy harvesting at both low and high frequencies. The R-FEG device consists of transistor-like multilayer blades to harvest kinetic energy of water at liquid-solid interface via bulk effect which is favorable at low frequency, and a magnetic rotor on symmetrical blade array to harvest rotational energy via electromagnetic effect at high frequency. As a result, the R-FEG device enables self-sustained operation at a wide range of flow rates, collectively delivering an enhanced power of 1131.3μW at a typical flow rate of 2.0 L/min. Moreover, the R-FEG exhibits potential versatility as a battery-independent power solution for environmental sensing and outdoor electronics by harvesting water energy across fluctuating flow regimes. This work provides a prospective prototype for water flow energy harvesting, paving a new avenue for scalable, maintenance-free power solutions for applications in remote, offshore, and distributed water energy harvesting.

Introduction

Electricity is the cornerstone of modern society, powering technologies integral to daily life and industrial progress. However, the escalating global energy demand, coupled with the environmental toll of fossil fuel-based power generation, underscores the imperative to transition toward renewable energy systems.[1] Among renewable sources, water energy stands out due to its ubiquity and untapped potential.[2-4] Traditional water energy harvesting that relies on bulky electromagnetic generator (EMG) can effectively harvest gravitational energy from centralized water reservoirs. However, abundant distributed low-frequency water energy stored in the forms of rain, streams, and rivers, remains largely untapped.

In 1867, Kelvin invented the water dropper and proved that water becomes charged when passed through and rubbed against a tube. Despite this discovery, effectively harvesting the electric charges at the time proved to be a significant challenge.[5] Recent decades have witnessed a surge in triboelectric nanogenerators (TENG),[6-10] which proven to be a promising alternative for decentralized water energy harvesting by harnessing the triboelectrification and electrostatic induction to convert low-frequency water flow into electricity with high voltage output.[11-15] Notably, water's fluidity enables unique liquid-solid interfacial interactions, expanding charge transfer efficiency beyond rigid solid-solid contact. Among myriad of TENG for water energy harvesting, *Xu et al* reported a droplet-based electricity generator (DEG) with bulk effect that utilizes hydrophobic surfaces and transistor-like electrode architectures to amplify charge separation and high-power densities.[16] The reported DEG has shown a promising perspective in collecting energy from different forms of water, such as rainwater,[17-22] rivers, and ocean waves,[23-28] establishing a new paradigm shift for decentralized water energy harvesting. Despite intensive progress, DEGs face limitations in sustaining continuous output under real-world conditions, particularly when harvesting energy from dynamic, low-frequency water flows.[29-32]

In this work, inspired by classical waterwheel that can spatially decouple the gravitational force of flowing water into orthogonal directions for continuous rotation, we report a R-FEG that enables continuous and efficient water energy harvesting at both low and high frequencies by integrating bulk effect of DEG and electromagnetic effect of EMG. By spatially decoupling the gravitational force of flowing water into two orthogonal directions, the kinetic energy of the flowing water is mainly converted into two parts: the kinetic energy of water film motion

a. *Department of Mechanical Engineering, The Hong Kong Polytechnic University, Hong Kong 999077, China. E-mail: zk.wang@polyu.edu.hk, baoping.zhang@polyu.edu.hk*
b. *Department of Mechanical Engineering, City University of Hong Kong, Hong Kong 999077, China*
c. *State Key Laboratory of High-performance Precision Manufacturing, Dalian University of Technology, Dalian 116024, P. R. China*
d. *Department of Electrical and Electronic Engineering, The Hong Kong Polytechnic University, Hong Kong, 999077, China*
† Electronic supplementary information (ESI) available. See DOI: 10.1039/x0xx00000x

View Article Online
DOI: 10.1039/D5LC00476D

on the wheel blade surface, and the kinetic energy of the wheel rotation. The R-FEG device consists of a DEG module that harnesses transistor-like multilayer engineered blades to harvest kinetic energy of water film motion via bulk effect (Classical waterwheel can't utilize this part energy) at low frequency, and an EMG module that utilizes magnetic rotor on symmetrical blade array to harvest rotational energy via electromagnetic induction at high frequency. The resulting R-FEG device demonstrates self-sustained operation at a wide range of flow rates, which delivers a collective high-power density featuring enhanced voltage output and current, capable of continuously powering up lamps and sensors. By simultaneously harvesting water energy from both liquid-solid surface contact and rotation, this work provides a prospective prototype for water flow energy harvesting, paving a new avenue for scalable, maintenance-free power solutions for applications in remote, offshore, and distributed water energy harvesting.

Results and discussion

Structural design and fabrication of R-FEG

Fig.1a illustrates the structural design of the R-FEG device, which integrates two distinct energy harvesting modules. One is a transistor-like DEG module that comprises 12 individual blades engineered with multilayer architecture consisting of a fluorinated ethylene propylene (FEP) as the dielectric layer and an Au electrode. In this DEG module, the flowing water acts as the primary energy source for efficient harvesting kinetic energy of water film motion via bulk effect. Upon contacting the top electrode, the water dynamically bridges the spatially separated top and bottom electrodes, enabling efficient charge transfer and amplifying electrical output through electrostatic induction. Analogous to a transistor configuration (Fig. S1), the bottom electrode functions as the source, the top electrode as the drain, and the impacting water acts as the gate. The second is an EMG module that employs a magnetic rotor mounted on a symmetrical blade array to harvest rotational energy via electromagnetic induction. Driven by water flowing, the coupled rotor and blades convert mechanical rotation into electrical energy through magnetic flux cutting.

The hydrodynamic interaction mechanism underlying R-FEG is elucidated in Fig. 1b. Upon a water column contacts the blade surface, gravitational forces resolve into two orthogonal

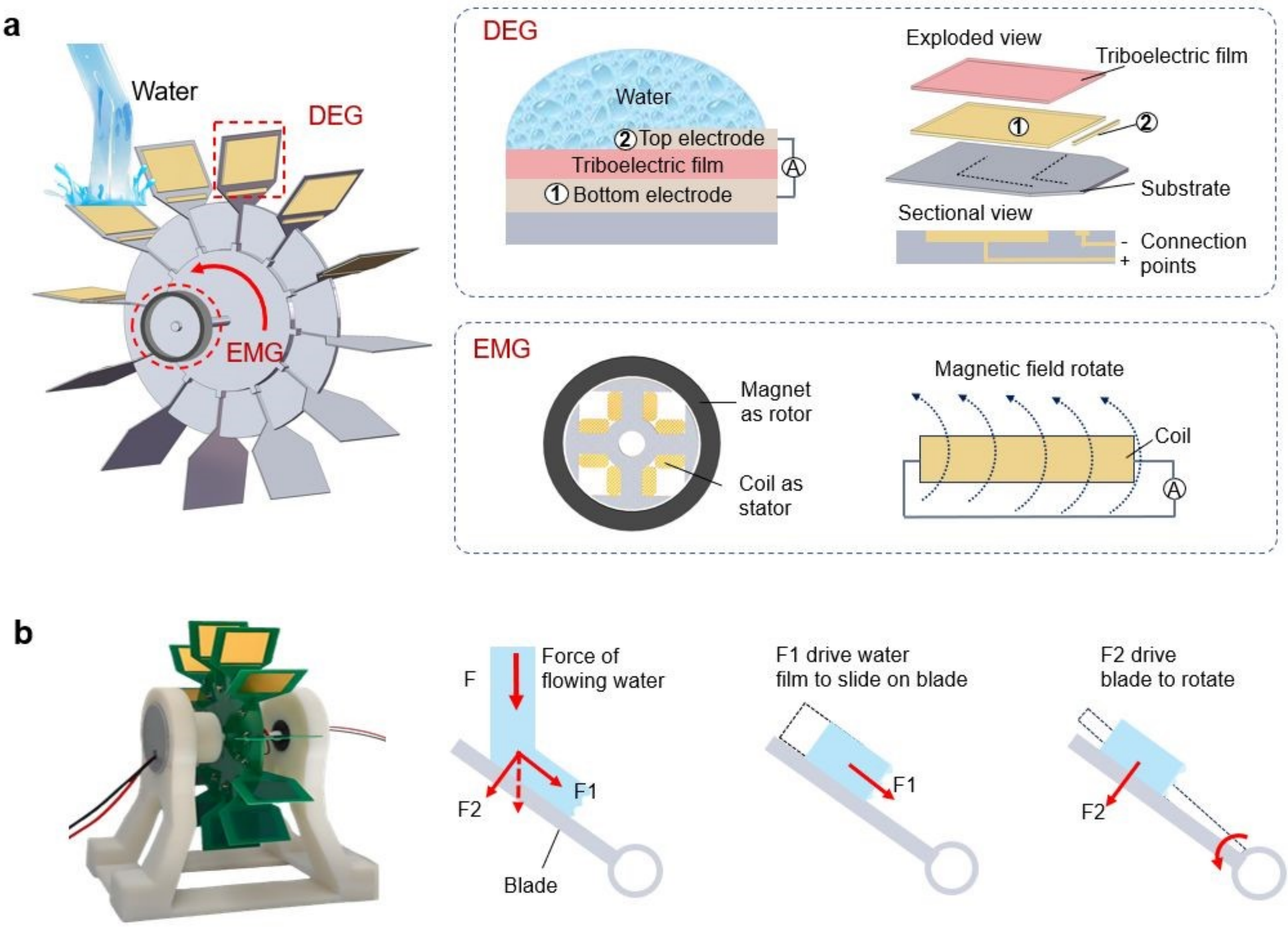

Fig. 1 Structural design of R-FEG. (a) Schematic illustration of the R-FEG device integrating a transistor-like DEG module that harnesses multilayer blades to harvest kinetic energy of water film motion via bulk effect and an EMG module that employs magnetic rotor on symmetrical blade array to harvest rotational energy via the electromagnetic effect. (b) R-FEG device with flowing water that splits gravitational force of water flow into two orthogonal directions by blade. The tangential component drives water-film sliding across the hydrophobic FEP layer for triboelectrification, while the normal component induces rotational torque for blade and rotor actuation.

‹x

View Article Online
DOI: 10.1039/D5LC00476D

components: a tangential force parallel to the blade surface induces lateral sliding of a thin water film across the hydrophobic FEP layer (Video S1), thereby initiating triboelectrification through liquid-solid interfacial interaction. Concurrently, the perpendicular force component generates rotational torque, driving both blade rotation and rotor actuation for electromagnetic induction. This dual-action design simultaneously harvests traditionally underutilized triboelectric energy from the sliding water film (via the DEG) at low frequency and rotational electromagnetic energy (via the EMG) at high frequency, achieving simultaneous multi-modal energy conversion.

Working mechanism of R-FEG

Fig. 2 demonstrates the electricity generation mechanism of transistor-like DEG module with bulk effect. The DEG module operates through liquid-solid triboelectrification, employing a transistor-like architecture to optimize interfacial charge transfer by bulk effect. As depicted by the circuit model of a single DEG unit (Fig. S2), the interaction between water flow and the FEP dielectric surface generates an interfacial electrical double layer (EDL) capacitor. Here, the DEG can be regarded as three capacitors: *Cf* (the FEP dielectric layer between its upper surface and the bottom electrode), *C1* (EDL capacitor at the water/FEP interface), and *C2* (EDL capacitor at the water/top electrode interface), with water itself functioning as a resistor in this circuit. In the initial state ("switch-off" state, Fig. S2), water flow impacts the FEP surface without bridging the top electrode, leaving the circuit open. Here, negative surface charges stored on the FEP electrostatically induce positive charges on the bottom electrode, yet no charge transfer occurs due to the absence of a conductive pathway. When the spreading water film connects the top electrode ("switch-on" state, Fig. S2), *C2* forms instantaneously, closing the circuit and initiating charge transfer.

Specifically, the triboelectric charge transfer process in DEG involves four distinct stages (Fig. 2a): Pre-contact (Step 1): Before water contacts the FEP surface, electrostatic induction localizes positive charges on the bottom electrode, counterbalancing the inherent negative charges on the FEP surface. Spreading initiation (Step 2): As the water film spreads, the expanding contact area between water and FEP increases, amplifying charge induction and transferring positive charges to the water film. Circuit closure (Step 3): When the water film spreads to bridge the top electrode and FEP, the electrostatically induced voltage on the bottom electrode generates an electric field, which drives positive charges from the bottom electrode to the top electrode, producing a power output. Retraction and reset (Step 4): During water film retraction, the diminishing contact area between the water and FEP reduces the induced charge density. This decline in electrostatic induction reverses the charge flow, causing positive charges to migrate back to the bottom electrode. Complete detachment of the water film from

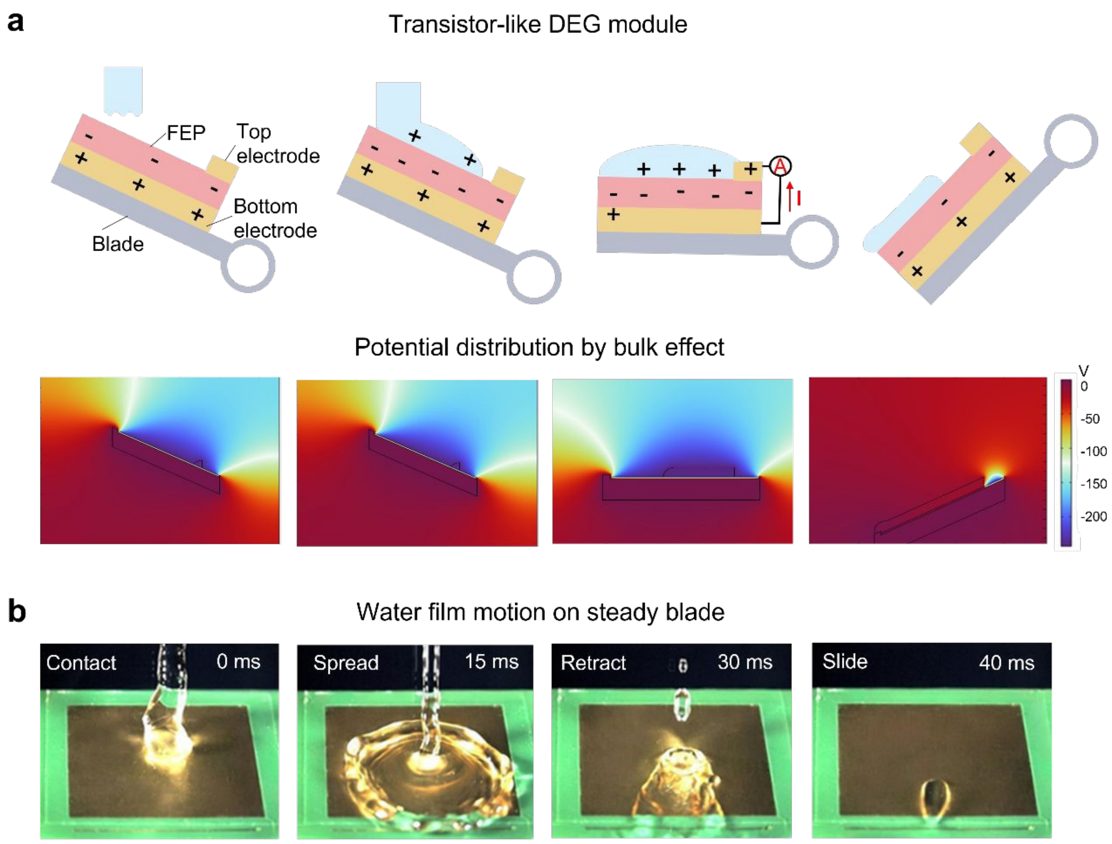

Fig. 2 The working mechanism of the transistor-like DEG module. (a) Schematically illustrating the triboelectric energy conversion in the DEG module and the simulated potential distribution. (b) Dynamic water film motion on steady blade.

View Article Online
DOI: 10.1039/D5LC00476D

the top electrode reopens the circuit, restoring all charges to their original state and preparing the system for the next cycle. This mechanism is further verified by the numerical simulation on potential distribution across the DEG (Fig.2a) and the corresponding dynamic water film motion is illustrated in Fig. 2b. To mitigate the effects of negative voltage fluctuations during charge reversal, the output of the rotary DEG is rectified using a full-wave bridge rectifier. This component converts the alternating current generated during water impact and retraction into a unidirectional direct current ensuring stable power delivery for practical applications.

Synchronized with the DEG module, the EMG module harvests rotational kinetic energy via electromagnetic induction. Specifically, when water flow impacts the blade surface, the perpendicular force drives the rotation of both the waterwheel and the attached magnet rotor. This rotation causes the magnetic flux lines to spin, enabling the stationary stator coils to cut through the changing magnetic field. According to Faraday's law ($E = -d\Phi/dt$), the electromotive force E induced in the coils is directly proportional to the rate of change of magnetic flux(Φ) over time (t) intercepted by the coil windings. To adapt the alternating current output for practical applications, the EMG employs diode-based rectification, converting the oscillating alternating current signal into a unidirectional direct current.

Electricity generation performance

We further demonstrate the continuous and efficient water energy harvesting performance of the R-FEG device. The rotary DEG module generated a peak short-circuit current of 15.27 μA and a peak open-circuit voltage of 43.5 V at a low flow rate of 1.0 L/min, representing fivefold and fourfold increase respectively over stationary counterparts (Fig. S3). This underscores the critical role of rotational motion in enabling continuous charge transfer and sustained output. Moreover, as shown in Fig.3a the output performance of rotary DEG module increases with the increment of flow rates, delivering both a peak voltage reaching 52.1 V and current 32.8 μA at a flow rate of 2.0 L/min. This flow-rate-dependent output performance can be further verified by the significant increase in voltage and current signal density (Fig. S4). The flow-rate-dependent output performance is attributed to the enhanced mechanical energy input at high-frequency flow rates, which amplifies both the contact area and the sliding velocity of the water film across the FEP surface, thereby intensifying electricity generation.

In addition to the flow rate, the output performance of the rotary DEG module exhibits pronounced dependence on the bottom electrode material and thickness of FEP. Specifically, compared to the traditional copper bottom electrode, rotary DEG module utilizing a nanostructured gold layer results in a twofold enhancement in peak current output (Fig. S5a), owing to its superior electron transfer ability and oxidation resistance. Meanwhile, reducing FEP dielectric thickness from 50 μm to 30 μm yields a higher open-circuit voltages due to enhanced capacitive coupling (Fig. S5b). Based on these optimization, Fig. 3b further demonstrates the output power of the rotary DEG module under different resistances of the external load at the typical flow rate of 2.0 L/min, delivering a peak instantaneous power (256 μW) at a 2.0 MΩ load.

Equally important, the EMG module of R-FEG demonstrates flow rate-dependent performance. Fig. 3c illustrates the peak open-circuit voltage and short-circuit current of EMG in relationship with flow rate. Specifically, initial operation at a low rate of 1.0 L/min yields fluctuating outputs with a peak output voltage and current of 0.3 V and 3.48 μA (Fig. S6), while progressive flow increment leads to enhanced performance, in terms of voltage, current, and signal density (Fig. S7-S9). At the flow rate of 2.0 L/min, the current output of EMG module achieves 4.32 mA. This is consistent with Faraday's law of induction, where increasing the flow rate elevates the rate of magnetic flux cutting, thereby boosting electromotive force. Fig. 3d shows that the optimum load resistance of EMG is 300 Ω, delivering a peak instantaneous power of 822.3 μW (flow rate 2.0 L/min). These results underscore the EMG's complementary role in delivering low-voltage but high-current output profile in relatively high-frequency water flow regimes.

Harnessing the complementary operation of DEG and EMG modules, the integrated R-FEG device achieves scalable energy harvesting with rectified combined output (Fig. 3e). Typically, a compact prototype (15×13×19 cm, 0.0037 m^3) exhibits flow-proportional power generation, delivering a high power of 1131.3μW (DEG contributes 21.8%) at 2.0 L/min (Fig. 3f). More contribution can be made by DEG especially in lower flow rate. The calculated energy conversion efficiency of R-FEG is 6.8%, which is higher than the previous reports (Table S1). The combination that integrates the DEG's electricity generation capability in low-frequency water flows with the EMG module's efficiency at high-frequency further endows the R-FEG with efficient energy harvesting across a wide range of water flow conditions.

Application demonstration

The modular design of R-FEG enables scalable deployment of water flow energy harvesting across diverse scenarios such as rainwater, tap water, small waterfalls, and streams (Fig. 4a). Typically, the compact small-scale R-FEG prototype demonstrates vast practical utilities in real-world applications. Fig. 4b shows that it can continuously light a 30cm long lamp by harvesting the triboelectric energy from a low position water flow 10 cm above the wheel blades at a rate of 2.0 L/min (Video S2). Also, the R-FEG can continuously power a lamp by harvesting water flow energy from tap water (Fig. 4c, video S3) and from an artificial waterfall in a park (Fig. S10, Video S4). We further demonstrate that R-FEG can be used as a power supply for monitoring sensors by sustaining real-time temperature/humidity sensing under flowing water (Fig. 4d, Video S5), validating its potential as a decentralized energy solution for distributed IoT networks in remote, off-grid environments. More interestingly, the R-FEG demonstrates its capacity for powering low-power electronics, such as a calculator (Fig. 4e, Video S6) and liquid-crystal displays (LCDs) that can enable dynamic environmental signage through alternating display modes under continuous flow conditions (Fig. 4f, Video S7). Such programmable alternating activation of

View Article Online
DOI: 10.1039/D5LC00476D

screen segments, displaying dynamic text or symbols, enables real-time environmental messaging, a feature applicable to public engagement in eco-sensitive areas. In addition, capacitor charging tests of R-FEG reveal rapid charging speed and efficiency (Fig. 4g), achieved by combining the rotary DEG's high-voltage triboelectric pulses with the EMG's sustained electromagnetic current. In addition, the DEG also shown durability (Fig. S11,12), ensuring long-term output for the R-FEG. This dual-module integration enables stable energy harvesting across fluctuating flow regimes, positioning the R-FEG as a versatile solution for off-grid monitoring and outdoor instrumentation without reliance on batteries or wired infrastructure.

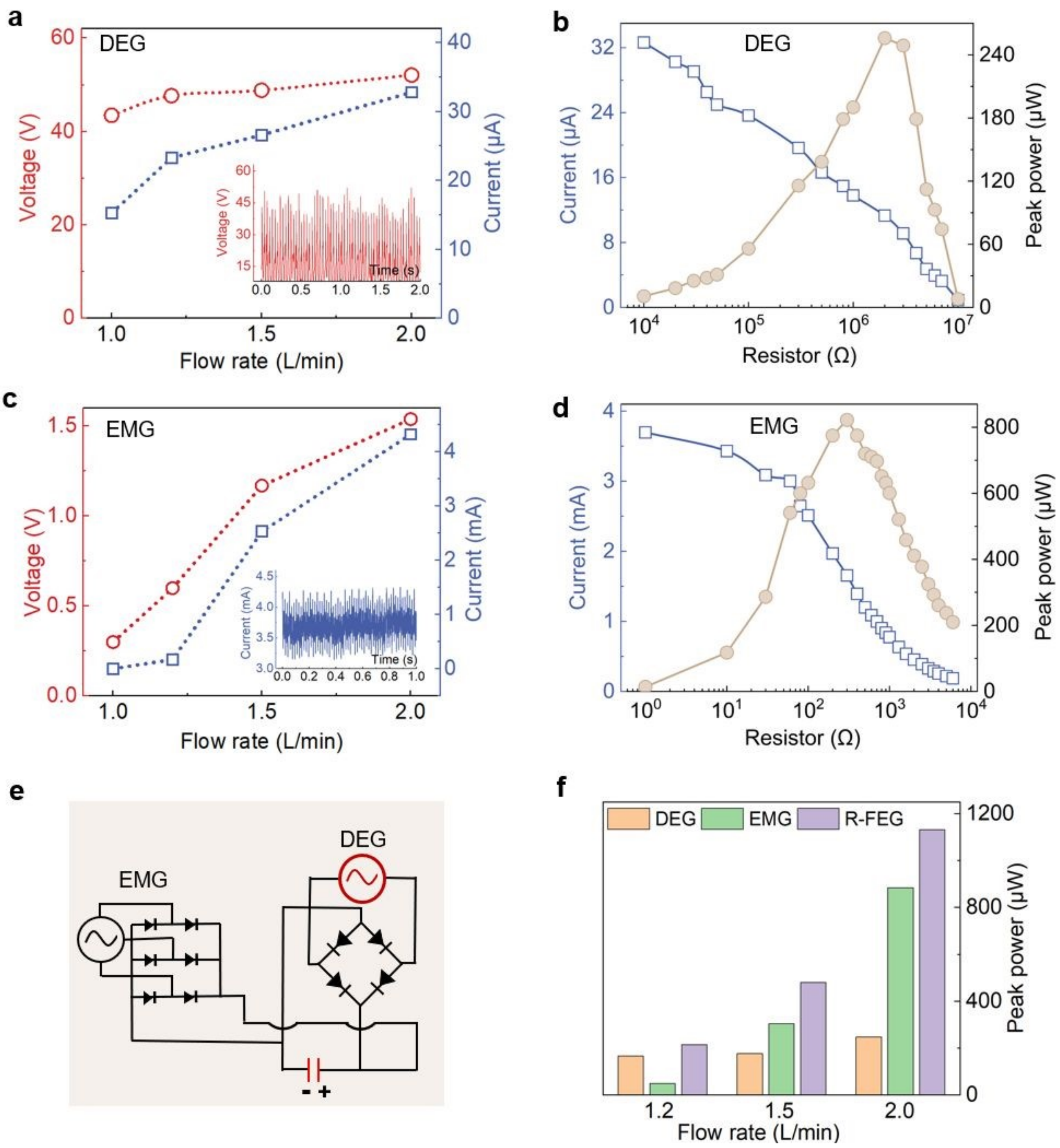

Fig. 3 Output performance of the R-FEG. (a) The DEG module's peak open-circuit voltage and short-circuit current increases with the flow rate. (b) The load current and load power of the rotary DEG versus load resistances. (c) The peak open-circuit voltage and short-circuit current of the EMG increases with the flow rate. (d) The load current and load power of the EMG versus load resistance. (e) Schematic illustrating the rectification circuit integrating outputs from DEG and the EMG modules. (f) The integrated peak power of R-FEG increases with the flow rate.

View Article Online
DOI: 10.1039/D5LC00476D

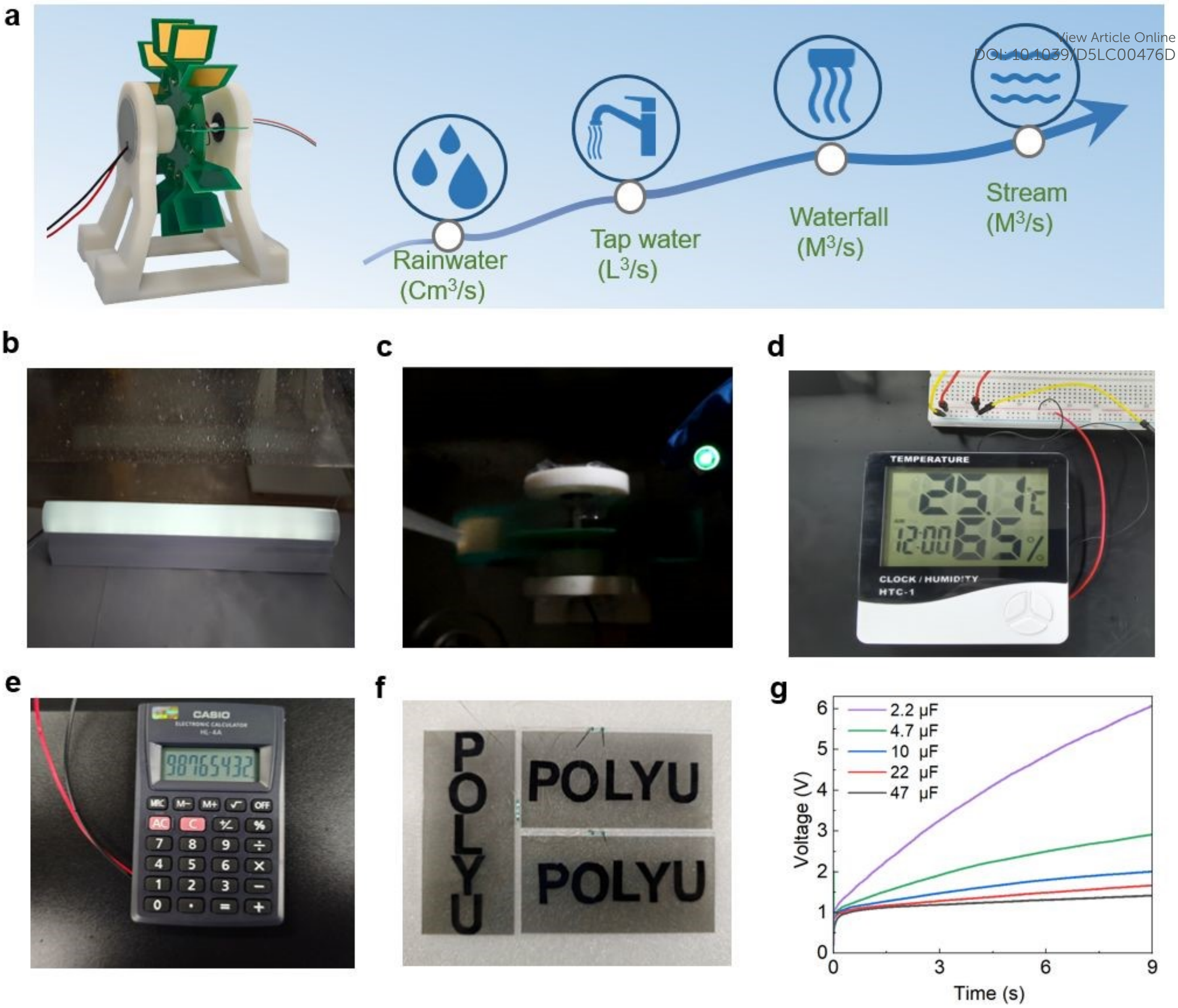

Fig. 4 Applications demonstrations of the R-FEG. (a) Optical image of the assembled R-FEG and its potential for scalable deployment of water flow energy harvesting across diverse scenarios such as rainwater, tap water and streams. (b) The rotary DEG continuously lights up a 30cm long lamp under low-flow conditions. (c) Tap water energy harvesting. (d) The R-FEG powers a real-time temperature and humidity sensing. (e) The R-FEG powers a calculator operation. (f) R-FEG powers three LCDs. (g) Capacitor charging curves demonstrate rapid charging speed powered by the R-FEG device.

Experimental

Materials and devices

FEP film is purchased from Shanghai Witlan Industry Co.,Ltd. An electric brush (MT0522-S06-WB, Shenzhen Moflon Technology Co., Ltd) is installed on one side of the center shaft to output the current of the R-FEG's DEG module effectively during rotation movement. An electric water pump is used to produce the water flow to drive the generator. During experimentation, water was released from a low position of 10 cm above the wheel blades, replicating low-frequency environments to quantify output characteristics. We recorded water's motion of spreading and retraction on a steady blade using a high-speed camera (iX Cameras i-SPEED 7) at a typical recording speed of 5,000 frames per second.

Fabrication of the R-FEG

The DEG module of R-FEG's consists of a rotation wheel (diameter:100mm) with 12 blades (width:3cm, length:3cm, embedded with a multilayer structure). The fabrication of the blade initiates with the deposition of a 30 nm-thick gold nanolayer onto the upper surface of the substrate, serving as the bottom electrode. Each blade surface is first cleaned with ethanol, after the evaporation of ethanol then taped with one triboelectric layer of fluorinated ethylene propylene (FEP) film (Thickness:

View Article Online
DOI: 10.1039/D5LC00476D

30μm). A microscale top electrode—comprising a 1 mm × 20 mm gold line—is precision-deposited near the edge of the blade's upper surface. Inside the substrate embedded with two miniature conductive pathways interconnect the bottom and top electrodes to designated positive (+) and negative (-) terminal points. This design minimizes wiring complexity while enabling scalable array output by interlinking the electrodes of the multi-piece blades via terminal points. The EMG module of R-FEG features a lightweight neodymium iron boron (NdFeB) permanent magnet ring (diameter: 29.2mm, height:10mm, thickness:1.6mm) in a casing (diameter:31mm) serving as the rotor, mechanically coupled to the central axis of the DEG module, while the stator (nine copper coils, turns: 380; height: 10.8mm) houses within an insulated shell. Finally, the hybrid nanogenerator was assembled on two coaxially 3D printed supports to ensure alignment and stability.

Electrical measurement

The output voltage and current performance of the devices were measured by an oscilloscope (Rohde and Schwarz RTE 1022) and a current preamplifier (Stanford Research Systems Model SR-570). All the experiments were conducted under the ambient relative humidity of 60% and ambient temperature of 26℃.

Conclusions

In summary, we developed a rotatable flowing water-based energy generator that integrates triboelectric and electromagnetic effects for continuous and efficient water energy harvesting. Our design is inspired by classical waterwheels, which spatially decouple the gravitational force of flowing water into orthogonal directions for continuous rotation. The designed R-FEG device consists of transistor-like multilayer structure engineered blades to harvest kinetic energy of water film motion at liquid-solid interface via bulk effect, and a magnetic rotor on symmetrical blade array to harvest rotational energy via electromagnetic induction. The R-FEG device enables self-sustained operation at a wide range of flow rates, collectively delivering an enhanced power of 1131.3μW at a typical flow rate of 2.0 L/min. Harnessing the complementary operation of DEG and EMG modules, the integrated R-FEG system enables scalable and sustainable water energy harvesting across fluctuating flow regimes, demonstrating its viability as a battery-independent power solution for off-grid environmental sensing and outdoor electronics. This work establishes a scalable, maintenance-free prototype for flowing water energy harvesting, paving new avenue for decentralized power generation in remote, offshore, and distributed water energy harvesting.

Author contributions

Hongbo Wang: Conceptualization, Methodology, Formula analysis, Investigation, Writing – original draft. Hangchen Liu: Resources, Methodology, Simulation. Yuxin Song: Resources, Investigation, Formula analysis. Xuezhi Qin: Resources, Investigation. Yang Li: Resources, Formula analysis. Kairui [12-15]Tang: Resources, Investigation. Huanxi Zheng: Conceptualization, Resources. Wanghuai Xu: Resources, Investigation. Zuankai Wang: Conceptualization, Methodology, Supervision, Writing – review & editing. Baoping Zhang: Methodology, Resources, Supervision, Writing–original draft, Writing– review & editing.

Conflicts of interest

There are no conflicts to declare.

Data availability

The data supporting this article have been included as part of the ESI.†

Acknowledgements

We acknowledge financial support from the National Natural Science Foundation of China (no. T2293694, no. 52333015), Research Grants Council of Hong Kong (no. 11215523, no. SRFS2223-1S01, no. N_PolyU5172/24, no. 15237824), the National Key Research and Development Program of China (no. 2023YFE0209900), the Innovation and Technology Commission of Hong Kong (no. MHP/025/23), Meituan Foundation through the Green Tech Award, and Research Grants of Hong Kong Polytechnic University (P0052886).

References

1. D. Welsby, J. Price, S. Pye and P. Ekins, *Nature*, 2021, **597**, 230-234.
2. B. Zhang, W. Xu, L. Peng, Y. Li, W. Zhang and Z. Wang, *Nature Reviews Electrical Engineering*, 2024, **1**, 218-233.
3. L. X. Li, X. Wang, W. Deng, J. Yin, X. M. Li and W. L. Guo, *Droplet*, 2023, **2**.
4. Z. M. Lin and Z. B. Yang, *Droplet*, 2024, **3**.
5. Y. Li, X. Z. Qin, Y. W. Feng, Y. X. Song, Z. R. Yi, H. X. Zheng, P. Y. Zhou, C. Y. Wu, S. Y. Yang, L. L. Wang, P. G. Zhu, W. H. Xu and Z. K. Wang, *Droplet*, 2024, **3**.
6. C. S. Wu, A. C. Wang, W. B. Ding, H. Y. Guo and Z. L. Wang, *Advanced Energy Materials*, 2019, **9**.
7. H. X. Hong, Y. W. Hu, C. S. Liu, C. Y. Wang, S. X. Chen, Z. Y. Zeng, C. S. Yan and H. Wu, *Chemical Engineering Journal*, 2025, **509**.
8. D. Y. Jiang, M. Y. Xu, M. Dong, F. Guo, X. H. Liu, G. J. Chen and Z. L. Wang, *Renewable & Sustainable Energy Reviews*, 2019, **115**.
9. X. Liang, T. Jiang, Y. W. Feng, P. J. Lu, J. An and Z. L. Wang, *Advanced Energy Materials*, 2020, **10**.
10. H. Wu, N. Mendel, D. van den Ende, G. F. Zhou and F. Mugele, *Physical Review Letters*, 2020, **125**.
11. X. T. Xu, P. Y. Li, Y. T. Ding, W. H. Xu, S. Y. Liu, Z. M. Zhang, Z. K. Wang and Z. B. Yang, *Energy & Environmental Science*, 2022, **15**, 2916-2926.
12. Z. Ma, J. W. Ai, Y. S. Shi, K. Wang and B. Su, *Advanced Materials*, 2020, **32**.

View Article Online
DOI: 10.1039/D5LC00476D

13. Y. Chen, B. Xie, J. Y. Long, Y. C. Kuang, X. Chen, M. X. Hou, J. Gao, S. Zhou, B. Fan, Y. B. He, Y. T. Zhang, C. P. Wong, Z. A. K. Wang and N. Zhao, *Advanced Materials*, 2021, **33**.
14. J. J. Yu, X. X. Wei, Y. C. Guo, Z. W. Zhang, P. S. Rui, Y. Zhao, W. Zhang, S. W. Shi and P. H. Wang, *Lab on a Chip*, 2021, **21**.
15. Z. M. Lin, B. B. Zhang, H. Y. Guo, Z. Y. Wu, H. Y. Zou, J. Yang and Z. L. Wang, *Nano Energy*, 2019, **64**.
16. W. H. Xu, H. X. Zheng, Y. Liu, X. F. Zhou, C. Zhang, Y. X. Song, X. Deng, M. Leung, Z. B. Yang, R. X. Xu, Z. L. Wang, X. C. Zeng and Z. K. Wang, *Nature*, 2020, **578**, 392-396.
17. W. H. Xu, X. F. Zhou, C. L. Hao, H. X. Zheng, Y. Liu, X. T. Yan, Z. B. Yang, M. Leung, X. C. Zeng, R. X. Xu and Z. K. Wang, *National Science Review*, 2019, **6**, 540-550.
18. Z. H. Lin, G. Cheng, S. Lee, K. C. Pradel and Z. L. Wang, *Advanced Materials*, 2014, **26**, 4690-4696.
19. L. L. Wang, Y. X. Song, W. H. Xu, W. B. Li, Y. K. Jin, S. W. Gao, S. Y. Yang, C. Y. Wu, S. Wang and Z. K. Wang, *Ecomat*, 2021, **3**.
20. X. Wang, S. M. Fang, J. Tan, T. Hu, W. C. Chu, J. Yin, J. X. Zhou and W. L. Guo, *Nano Energy*, 2021, **80**.
21. F. Wen and C. Lee, *Droplet*, 2024, **3**.
22. H. Wu, N. Mendel, S. van Der Ham, L. L. Shui, G. F. Zhou and F. Mugele, *Advanced Materials*, 2020, **32**.
23. Z. L. Wang, *Nature*, 2017, **542**, 159-160.
24. J. An, Z. M. Wang, T. Jiang, X. Liang and Z. L. Wang, *Advanced Functional Materials*, 2019, **29**.
25. Z. H. Lin, G. Cheng, L. Lin, S. Lee and Z. L. Wang, *Angewandte Chemie-International Edition*, 2013, **52**, 12545-12549.
26. P. S. Rui, W. Zhang, Y. M. Zhong, X. X. Wei, Y. C. Guo, S. W. Shi, Y. L. Liao, J. Cheng and P. H. Wang, *Nano Energy*, 2020, **74**.
27. S. F. Leung, H. C. Fu, M. L. Zhang, A. H. Hassan, T. Jiang, K. N. Salama, Z. L. Wang and J. H. He, *Energy & Environmental Science*, 2020, **13**, 1300-1308.
28. D. H. Zhang, J. W. Shi, Y. L. Si and T. Li, *Nano Energy*, 2019, **61**, 132-140.
29. S. Y. Jin, Y. X. Wang, M. Motlag, S. J. Gao, J. Xu, Q. Nian, W. Z. Wu and G. J. Cheng, *Advanced Materials*, 2018, **30**.
30. J. Park, Y. Yang, S. H. Kwon and Y. S. Kim, *Journal of Physical Chemistry Letters*, 2015, **6**, 745-749.
31. Y. X. Song, W. H. Xu, Y. Liu, H. X. Zheng, M. M. Cui, Y. S. Zhou, B. P. Zhang, X. T. Yan, L. L. Wang, P. Y. Li, X. T. Xu, Z. B. Yang and Z. K. Wang, *Innovation*, 2022, **3**.
32. H. Wu, S. Wang, Z. K. Wang and Y. L. Zi, *Nature Communications*, 2021, **12**.

View Article Online
DOI: 10.1039/D5LC00476D

ARTICLE

A hybrid flowing water-based energy generator inspired by rotatable waterwheel

Received 00th January 20xx,
Accepted 00th January 20xx

DOI: 10.1039/x0xx00000x

Hongbo Wang,[a] Hangchen Liu,[a] Yuxin Song,[a] Xuezhi Qin,[b] Yang Li,[b] Kairui Tang,[a] Huanxi Zheng,[c] Wanghuai Xu,[d] Zuankai Wang*[a] and Baoping Zhang*[a]

Data availability

The data supporting this article have been included as part of the ESI.†

[a.] *Department of Mechanical Engineering, The Hong Kong Polytechnic University, Hong Kong 999077, China. E-mail: zk.wang@polyu.edu.hk, baoping.zhang@polyu.edu.hk*
[b.] *Department of Mechanical Engineering, City University of Hong Kong, Hong Kong 999077, China*
[c.] *State Key Laboratory of High-performance Precision Manufacturing, Dalian University of Technology, Dalian 116024, P. R. China*
[d.] *Department of Electrical and Electronic Engineering, The Hong Kong Polytechnic University, Hong Kong, 999077, China*
† Electronic supplementary information (ESI) available. See DOI: 10.1039/x0xx00000x